Development 136, 3413-3421 (2009) doi:10.1242/dev.036061

H19 acts as a trans regulator of the imprinted gene network controlling growth in mice

Anne Gabory[1], Marie-Anne Ripoche[1], Anne Le Digarcher[2], Françoise Watrin[3], Ahmed Ziyyat[1], Thierry Forné[4], Hélène Jammes[5], Justin F. X. Ainscough[6], M. Azim Surani[7], Laurent Journot[2] and Luisa Dandolo[1,*]

The imprinted *H19* gene produces a non-coding RNA of unknown function. Mice lacking *H19* show an overgrowth phenotype, due to a cis effect of the *H19* locus on the adjacent *Igf2* gene. To explore the function of the RNA itself, we produced transgenic mice overexpressing *H19*. We observed postnatal growth reduction in two independent transgenic lines and detected a decrease of *Igf2* expression in embryos. An extensive analysis of several other genes from the newly described imprinted gene network (IGN) was performed in both loss- and gain-of-function animals. We found that *H19* deletion leads to the upregulation of several genes of the IGN. This overexpression is restored to the wild-type level by transgenic expression of *H19*. We therefore propose that the *H19* gene participates as a trans regulator in the fine-tuning of this IGN in the mouse embryo. This is the first in vivo evidence of a functional role for the *H19* RNA. Our results also bring further experimental evidence for the existence of the IGN and open new perspectives in the comprehension of the role of genomic imprinting in embryonic growth and in human imprinting pathologies.

KEY WORDS: *H19*, *Igf2*, Transgenic mouse models, Imprinted gene network (IGN), Genomic imprinting, Non-coding RNA

INTRODUCTION

The *H19* gene was cloned 20 years ago (Pachnis et al., 1988) and was one of the first imprinted genes to be identified. Genomic imprinting is an epigenetic mechanism that leads to parent-of-origin specific monoallelic expression. Thus, *H19* is expressed from the maternal allele in mouse and human (Bartolomei et al., 1991; Zhang and Tycko, 1992). The *H19* RNA is transcribed by RNA polymerase II, capped, polyadenylated and spliced, but it lacks conserved ORFs between human and mouse (Brannan et al., 1990). Its complex conserved predicted structure suggests that the functional product is a non-coding RNA (Juan et al., 2000). In addition, a microRNA (miR-675) has been recently described in the first exon of the gene (Cai and Cullen, 2007; Mineno et al., 2006). Both the full-length RNA and the miRNA have been identified in marsupials, suggesting a strong functional conservation throughout evolution (Smits et al., 2008). *H19* is strongly expressed during mouse embryogenesis in mesoderm and endoderm-derived tissues. Its expression is then fully repressed after birth and is found only in skeletal muscle and heart in adults (Poirier et al., 1991). This expression pattern is similar to that of the *Igf2* (insulin-like growth factor 2) gene, which is paternally expressed and encodes a major fetal growth factor (DeChiara et al., 1991).

Imprinted genes are associated with differentially methylated regions (DMRs), which are involved in the regulation of their expression. The *H19* and *Igf2* genes are linked on the distal part of mouse chromosome 7 and on the human 11p15.5 region (Zemel et al., 1992). The DMR located between 2- and 4-kb upstream of the *H19* gene is the imprinting control region (ICR) of the locus, as its deletion affects both *H19* and *Igf2* expression (Thorvaldsen et al., 1998). This sequence binds the insulator protein CTCF on the unmethylated maternal allele, thereby creating a boundary between the downstream enhancers and the *Igf2* maternal allele (Hark et al., 2000).

In order to decipher the role of the *H19* non-coding RNA, two knock-out models were established. In the first model, referred to as $H19^{\Delta 13}$, the 3-kb transcribed region and the 10 kb upstream of that region were deleted. In the second model, referred to as $H19^{\Delta 3}$, the 3-kb transcription unit only was deleted. In both models, the maternal heterozygous $H19^{\Delta mat/+}$ mice, which do not express the RNA, are viable, fertile and present an overgrowth phenotype. In $H19^{\Delta 13}$mice, the maternal *Igf2* allele is totally reactivated in all expressing tissues because of the deletion of the ICR (Leighton et al., 1995). In $H19^{\Delta 3}$ mice, expression of the maternal *Igf2* allele is 25% that of the paternal allele in wild-type mice, and is only observed in mesoderm derived tissues (skeletal muscle, tongue, diaphragm and heart) (Ripoche et al., 1997; Yoshimizu et al., 2008). The reactivation of the maternal *Igf2* allele in both *H19* targeted models is most probably due to a cis effect of an altered chromatin structure rather than to the lack of the *H19* RNA (for a review, see Gabory et al., 2006).

Different studies have lead to proposals of a role for the *H19* RNA itself. First, maternal transmission of the $H19^{\Delta 13}$ or $^{\Delta 3}$ deletion leads to modification of the methylation pattern of the *Igf2* gene DMRs in cis with hypermethylation of the maternal allele, but also in trans with hypomethylation on the paternal allele (Forne et al., 1997). Second, *H19* was found to be associated with polysomes in different human and mouse cell lines (Li et al., 1998; Milligan et al., 2000). Finally, after transfection of human DiHepG2 cells, *H19* was suggested to participate in IGF2 protein repression, in part through transcriptional regulation (Wilkin et al., 2000).

Another clue for the function of the *H19* gene is its implication in tumorigenesis. *H19* cDNA transfection into a cancer cell line results in loss of clonogenicity of the cells and reduced tumorigenicity in *nude* mice (Hao et al., 1993). Moreover, *H19*/*Igf2* locus imprinting is lost in Wilms' tumor resulting in *Igf2* biallelic expression and total

[1]Genetics and Development Department, Inserm U567, CNRS UMR 8104, University of Paris Descartes, Institut Cochin, Paris, France. [2]Institut de Genomique Fonctionnelle, CNRS UMR 5203, INSERM U661, University of Montpellier II, Montpellier, France. [3]Inserm U901-INMED, Parc scientifique de Luminy, Marseille, France. [4]Institut de Génétique Moléculaire de Montpellier, CNRS UMR 5535, University of Montpellier II, Montpellier, France. [5]PHASE Department, INRA, Jouy en Josas, France. [6]Leeds Institute of Genetics, Health and Therapeutics, University of Leeds, Leeds LS2 9JT, UK. [7]Wellcome Trust/Cancer Research UK Gurdon Institute of Cancer and Developmental Biology, University of Cambridge, Cambridge CB2 1QN, UK.

*Author for correspondence (luisa.dandolo@inserm.fr)

Accepted 11 August 2009

repression of *H19* (Dao et al., 1999; Frevel et al., 1999). Both observations suggest a tumor suppressor effect of *H19*. However, other in vitro studies suggest that *H19* acts as an oncogene and is activated by the *c-myc* transcription factor (Barsyte-Lovejoy et al., 2006; Matouk et al., 2007). Finally, we recently showed that *H19* acts in vivo as a tumor suppressor in three different mouse models (Yoshimizu et al., 2008). Targets of this tumor suppressor remain to be identified.

We decided to study the potential role of the *H19* RNA in vivo. We created a new *H19* transgenic line (Tg24) (Fig. 1A) and used the previously described YZ8 one-copy YAC line (Fig. 1B) (Ainscough et al., 1997). These lines were bred onto an $H19^{\Delta 3}$ background. Our aim was to rescue the $H19^{\Delta 3}$ phenotype with the *H19* transgenes in order to observe a trans effect of the RNA, independently of the cis effect observed on maternal *Igf2* transcription. We found that the overgrowth phenotype observed in $H19^{\Delta 3}$ animals compared with wild-type littermates is not present in $H19^{\Delta 3}$ mice expressing the transgenes, thus suggesting a rescue due to transgenic expression of *H19* RNA. We identified *Igf2* mRNA as one of the targets of *H19*. We then performed an extensive analysis of the expression of genes belonging to the recently described imprinted gene network (IGN) (Varrault et al., 2006). Our results indicate that alteration of the *H19* dosage modulates the expression of several other imprinted genes in this network, suggesting that *H19* acts as a trans regulator of the IGN.

MATERIALS AND METHODS

Transgene construction

We created several transgenic lines expressing the *H19* RNA under the control of the necdin (*Ndn*) gene promoter. *Ndn* is expressed in some non-neural tissues (somites, tongue, axial muscles), with a more specific expression in most postmitotic neurons of the central and peripheral nervous systems (Andrieu et al., 2003). A genomic 1.5-kb *Sac*I fragment containing the *Ndn* promoter (D76440) was isolated and inserted in the *Sac*I site of the pGEM3Zf(+) vector. A 4.3-kb *Dra*III genomic fragment containing the *H19* gene (AF04091) was further introduced in the *Sma*I-linearized *Ndn* promoter-pGEM3Zf(+) vector (Fig. 1A). The *Ndn* promoter-*H19* cassette was then excised by an *Eco*RI and *Sal*I digestion and introduced in an *Eco*RI/*Sal*I-linearized pBS vector. The upstream 2.3-kb *Eco*RI *Ndn* genomic fragment (containing conserved motifs between mouse and human) was inserted in the *Eco*RI site of this latter vector (Kuo et al., 1995). Orientation of this fragment was determined by PCR amplification. The *Ndn* promoter region was sequenced in order to avoid any mutation in this region. The hybrid 6.5-kb *Ndn-H19* mini-transgene was excised from the pBS vector by a *Not*I/*Sal*I digestion and agarose gel purified. The DNA was further purified on an ELUTIP-D column (Schleicher & Schuell, Germany), as described in the manufacturer's protocol, and was resuspended in injection buffer [10 mM Tris-HCl (pH 7.5), 0.1 mM EDTA (pH 8), 100 mM NaCl] at a final concentration of 2 ng/μl and microinjected into the pronucleus of C57BL/6×CBA fertilized eggs. Founders were identified by Southern blot analysis after *Hin*dIII digestion of tail DNA using an *Ndn* PCR-amplified probe (primers N8 and N28; see below; Fig. 1A′). Four founders were bred with C57BL/6×CBA females to establish the transgenic lines. Ectopic *H19* expression was then checked by breeding transgenic males with $H19^{\Delta 3}$ females. Only one line, subsequently named the Tg24 line, was kept, as the others displayed low or variegated expression of *H19*, as detected by in situ hybridization. Expression was found not only in the central nervous system, as was expected from the expression pattern of the endogenous *Ndn* gene, but also to be comparatively widespread, suggesting that the promoter region did not contain all of the regulatory control sequences present in the endogenous gene (see Fig. S1 in the supplementary material). Transgene copy number was determined by Southern blot analysis to be 30 copies (Fig. 1A′).

$H19^{\Delta 3}$, Tg24 and YZ8 one-copy YAC lines (Fig. 1B) were all maintained on a C57BL/6×CBA background and wild-type mice used for matings were C57BL/6×CBA. The protocol of animal handling and treatment was performed in accordance with the guidelines of the animal ethics committee of the Ministère de l'Agriculture of France.

Genotyping

DNA was extracted from tail biopsies and PCR was performed according to the manufacturer's instructions (Invitrogen). For the Tg24 line, primers N6 and N16, hybridizing to the *Ndn* promoter were used; a 1.5-kb transgenic fragment and a 2-kb *Ndn* endogenous fragment were obtained. For the YAC line, *lacZ* primers were used. *neo* primers were used to genotype the $H19^{\Delta 3}$ allele in heterozygous animals. Primer sequences and annealing temperature conditions are described in the section below.

Primers

Primers for genotyping

Annealing temperatures are given in parentheses.
Ndn (58°C), GCATCTTATTCATGAGAGAC (N8, sense) and CTCGGTGGAGACCAGCAG (N28, antisense);
Ndn (52°C), GCTCTCCATTTCTATTAGGTC (N6, sense) and GCAATATTTCTCTACAAGAC (N16, antisense);
neo (66°C), GTGTTCCGGCTGTCAGCGCA (sense) and GTCCTGATAGCGGTCCGCCA (antisense);
lacZ (55°C), CAGTTTACCCGCTCTGCTAC (sense) and GCGTTGGCAATTTAACCGCC (antisense).

Primers for qPCR

Annealing temperatures are given in parentheses.
H19 (60°C), GGAGACTAGGCCAGGTCTC (sense) and GCCCATGGTGTTCAAGAAGGC (antisense);
TBP (60°C), GCAATCAACATCTCAGCAACC (sense) and CGAAGTGCAATGGTCTTTAGG (antisense).

Gene expression analysis

Collected tissues were disrupted using a Mixer Mill (Qiagen) and total RNA was extracted with TRIzol reagent (Invitrogen), according to the manufacturer's instructions. Extracted RNA was RQ1-DNase treated (Promega) and then re-extracted with phenol:chloroform and chloroform before ethanol precipitation.

For the expression profile analysis, we carried out reverse transcription with SuperScriptII (Invitrogen) on 500 ng of total RNA with random hexamer oligonucleotides. Quantitative PCR was performed for *H19* and TATA-binding protein (*TBP*) genes on 1 ng cDNA in a final volume of 10 μl with FastStart Master Mix reagent in a Light-Cycler 2.0 system (Roche). Primer sequences are given above.

For the IGN analysis, RNA was prepared from two animals per genotype from two different litters; therefore, four animals per genotype for each mating were analyzed. We carried out three independent reverse transcription experiments for each sample on 1 μg of total RNA. qPCR was performed on 2 ng cDNA in a Light-Cycler 480 system (Roche). The primers used to amplify the imprinted genes have been described previously (Varrault et al., 2006). The selection of appropriate housekeeping genes was performed with geNorm (Vandesompele et al., 2002). The level of expression of each imprinted gene X was normalized to the geometric mean of the expression levels of several housekeeping genes (*Hprt2*, *Trfr1* and *Tubb2* for the transgenic line; *Gus2*, *Mrpl32*, *Hprt2* and *Tubb2* for the YAC line), according to the formula:

$$X / \text{geometric mean (R1, R2, R3)} = 2^{(Ct[X] - \text{arithmetic mean } [Ct(R1), Ct(R2), Ct(R3)])},$$

where Ct is the threshold cycle, and R1, R2, R3 are the three reference genes. Data were analyzed using a non-parametric Kruskal-Wallis one-way analysis of variance with Benjamini-Hochberg correction (FDR 5%) for multiple testing, as implemented in the MeV 4.2 package (www.tm4.org), followed by post-hoc paired comparisons.

Growth curve analysis

Newborn animals were marked at day 1 and weighed almost every day from birth to 4 weeks. Males and females were separated at 4 weeks and littermates of the same sex placed in the same cage in order to keep the same environment for the different genotypes during the rest of the experiment. The animals were then weighed twice a week up to 10 weeks. For each line, at least four litters were analyzed. Weights were plotted on growth curves and a two-factor (litter and genotype) Anova statistical analysis using StatView software was performed for each sex at each

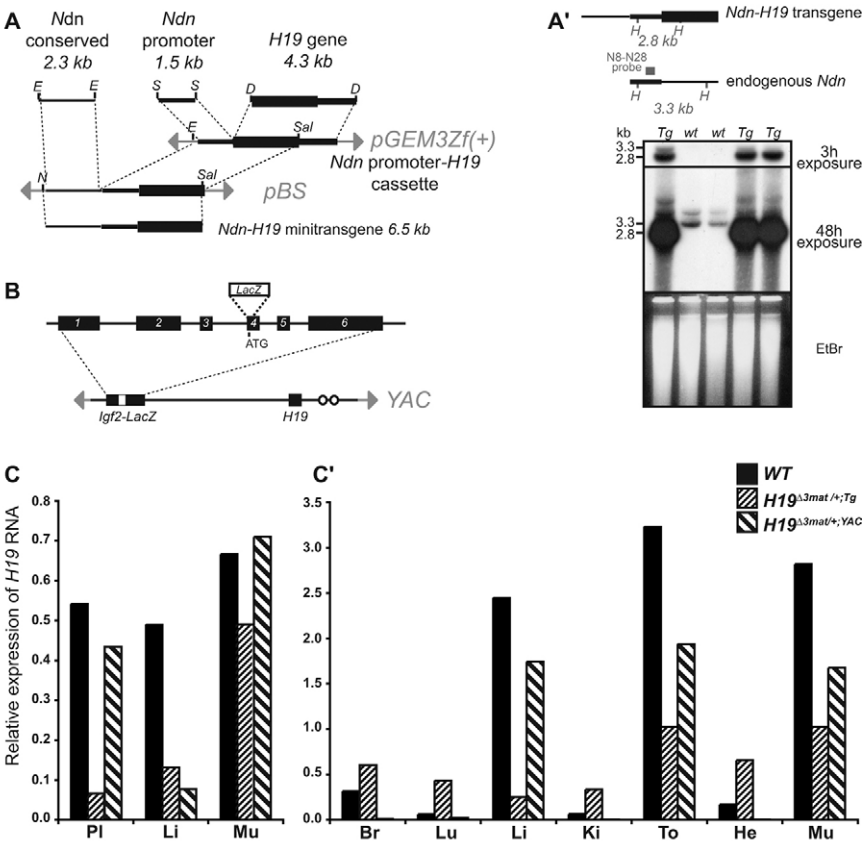

Fig. 1. Expression of *H19* in transgenic lines. (**A**) Tg24 line construct. A 2.3-kb *Ndn* conserved fragment and the minimal 1.5-kb *Ndn* promoter were placed upstream from the *H19* transcription unit to produce a 6.5-kb *Ndn-H19* transgene. Restriction sites: D, *Dra*III; E, *Eco*RI; N, *Not*I; S, *Sac*I; Sal, *Sal*I. (**A′**) Southern analysis of transgene integration in the Tg24 line on *Hin*dIII digested tail DNA. Position of the N8-N28 probe is indicated (grey square). Phosphoimager quantification showed the integration of 30 copies. H, *Hin*dIII. (**B**) YAC transgene construct (130 kb) as described by Ainscough et al. (Ainscough et al., 1997). *H19* is under the control of its own promoter and *Igf2* is replaced by a *lacZ* construct. The YZ8 line displays a one copy integration. (**C**,**C′**) The transgenes were bred on an $H19^{\Delta 3}$ background in order to detect transgenic *H19* expression alone. (C) Expression in E14.5 embryos. Pl, placenta; Li, liver; Mu, posterior limb muscle. (C′) Expression in P5 neonates. Br, brain; Lu, lung; L, liver; Ki, kidney; To, tongue; He, heart; Mu, skeletal muscle. *H19* expression is expressed in arbitrary units, relative to *TBP* gene expression. RT-qPCR experiments were carried out on pools of two samples from the same genotype.

point. The weight ratio of transgenic to control animals ($H19^{\Delta 3mat/+}$ or wild type) was calculated. This ratio was expressed as the percentage of transgenic animal weight versus control (Fig. 2B).

RESULTS

Pattern of expression of *H19* in transgenic animals

We first performed a detailed analysis of *H19* expression in both transgenic lines. Tg24 and YZ8 YAC mice were analyzed on the $H19^{\Delta 3}$ background, which meant that any resulting *H19* expression was of transgenic origin only. These two genotypes were compared with wild-type mice. Northern analysis was performed on RNA from Tg24 and wild-type embryos (whole embryos or liver and limb muscle from E10.5 to 18.5, and placentas from E12.5 to 18.5; see Fig. S1A in the supplementary material). Placenta, liver and limb muscle from E14.5 embryos from both Tg24 and YZ8 transgenic lines were chosen to precisely evaluate the levels of transgenic *H19* RNA by RT-qPCR (Fig. 1C). P5 neonatal pups were also dissected and brain, tongue, heart, lung, liver, kidney and muscle from posterior limbs were collected. RNA was prepared from these tissues and the level of expression of *H19* was evaluated both by northern analysis (see Fig. S1B in the supplementary material) and by RT-qPCR (Fig. 1C′). In embryos (Fig. 1C), *H19* was expressed in both transgenic lines and expression in posterior limb muscle was comparable to that in wild type. However, only low expression of *H19* was detected in embryonic liver; this was in contrast to previously published in situ hybridization YAC data, which showed high expression in liver (Ainscough et al., 2000a). In the YAC line, expression in the placenta was similar to that in wild type, whereas the Tg24 placenta expressed only low amounts of *H19* RNA.

In newborn Tg24 mice (Fig. 1C′), *H19* was transcribed at a lower level than wild type in liver, tongue and muscle, and at a higher level than wild type in brain, lung, kidney and heart. The expression profile of the YAC line was consistent with previously described data (Ainscough et al., 2000b), with a notable lack of expression in lung, kidney and heart, and strong expression in liver, tongue and muscle. Based on these results, we focused on E14.5 embryonic muscle for further analyses.

Phenotype of the transgenic lines

As both transgenic lines expressed *H19*, we closely observed their phenotype. The $H19^{\Delta 3}$ mutant displays an overgrowth phenotype. We therefore performed a meticulous analysis of growth in both transgenic lines to observe whether transgenic expression of *H19* could rescue the phenotype of the $H19^{\Delta 3}$ mutants. Mice were weighed for 10 weeks and weights were plotted on growth curves (Fig. 2A). At least four individual litters were followed over the 10-week period for each transgenic line. Each graph corresponds to the mean weight of these litters for each mating, females and males being separated. The ratio between transgenic and control genotypes for each sex was then calculated at each point from each litter. The average ratio for each mating is plotted on Fig. 2B. A ratio of 100% indicates that there is no difference between transgenic and control animals. We first compared the growth curves of $H19^{\Delta 3mat/+}$ and wild-type littermates. At birth, the $H19^{\Delta 3mat/+}$ mice have a significant 20% overgrowth phenotype, this overgrowth decreases to 4% at day 9, and then increases to 14% in the second week and remains stable (Fig. 2B).

$H19^{\Delta 3}$ females were mated with hemizygous Tg24 males in order to obtain $H19^{\Delta 3mat/+}$ and $H19^{\Delta 3mat/+;Tg24}$ animals in the same litter. We observed a growth restriction of $H19^{\Delta 3mat/+;Tg24}$ animals compared with their control $H19^{\Delta 3mat/+}$ littermates (Fig. 2A). The difference in weight between the two phenotypes was evident not only in the animals after weaning (as seen in Fig. 2A), but also before, as assessed by ANOVA statistical test, with a significant

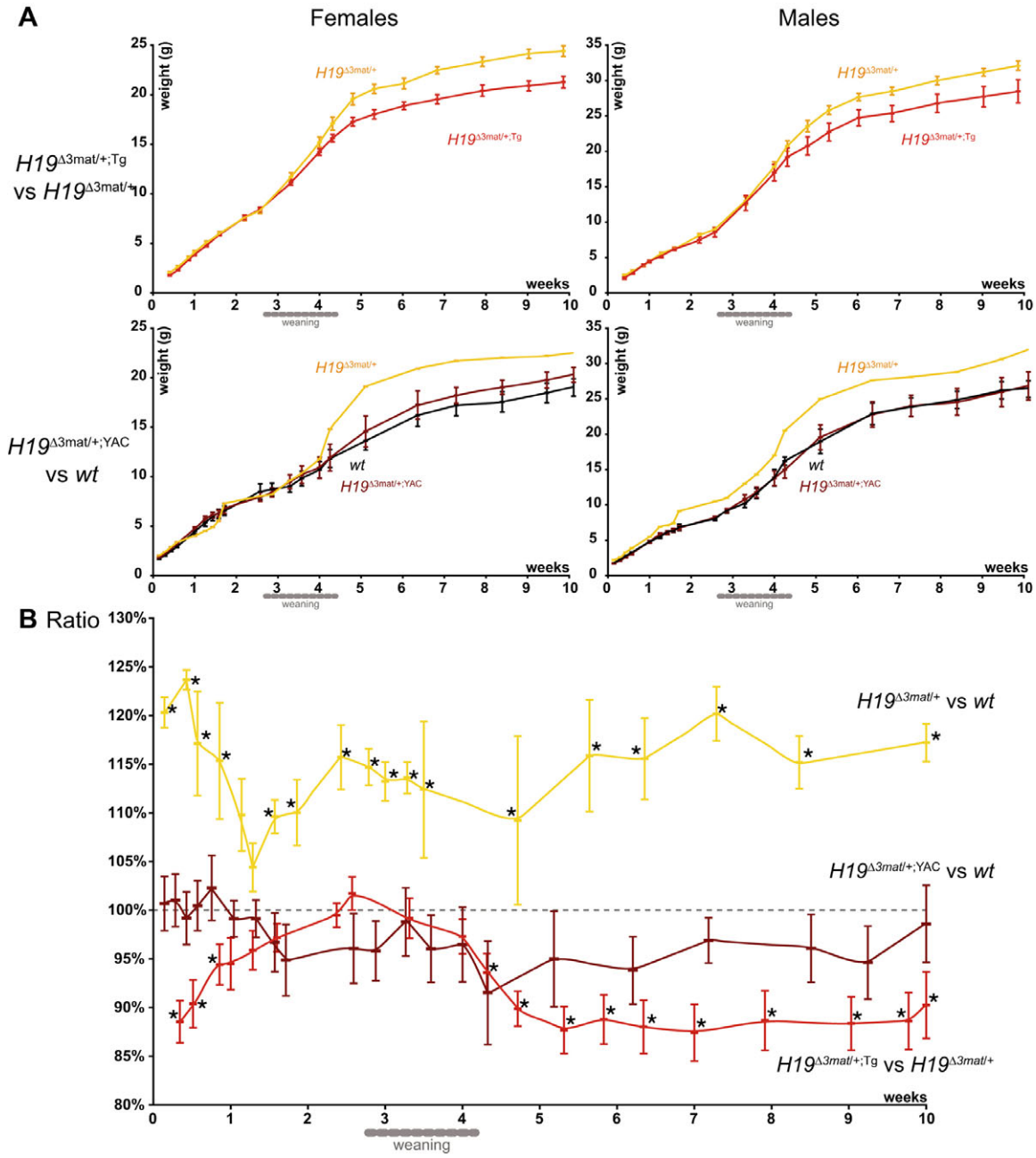

Fig. 2. Growth phenotype of the transgenic animals. (**A**) Growth curves for female (left) and male (right) littermates from $H19^{\Delta 3/\Delta 3}\times H19^{+/+;Tg24+/-}$ and $H19^{\Delta 3/+;YAC+/-}\times$wild type matings. Each growth curve represents the average weight of four litters. Error bars indicate s.e.m. (**B**) The graph represents the mean weight ratios of at least four littermates for each genotype over a period of 10 weeks. Error bars indicate s.e.m. A ratio of 100% indicates no difference in weight between genotypes.

difference being observed during the first week ($P<0.05$). At birth, the $H19^{\Delta 3mat/+;Tg24}$ mice weight was decreased by 11% compared with control $H19^{\Delta 3mat/+}$ littermates (Fig. 2B). Interestingly, the $H19^{\Delta 3mat/+;Tg24}$ mice had a weight similar to that of control mice during the second week. Subsequently, the weight difference increased again and after weaning the $H19^{\Delta 3mat/+;Tg24}$ mice presented an 11% decrease compared with control $H19^{\Delta 3mat/+}$ littermates. The opposite growth phenotypes of the $H19^{\Delta 3mat/+}$ and $H19^{\Delta 3mat/+;Tg24}$ mice suggest that the transgenic *H19* expression is able to rescue the $H19^{\Delta 3}$ overgrowth phenotype.

We then analyzed the YZ8 YAC transgenic line. As the YAC transgene is imprinted, it must be transmitted from the mother to obtain *H19* transgenic expression. $H19^{\Delta 3mat/+;YAC}$ females were first obtained and mated with wild-type males in order to obtain wild-type, $H19^{\Delta 3mat/+}$ and $H19^{\Delta 3mat/+;YAC}$ littermates. Unfortunately, we observed a bias in the litters and obtained only a few $H19^{\Delta 3mat/+}$ animals. Therefore wild-type and $H19^{\Delta 3mat/+;YAC}$ were used for the growth study; the growth curves for the single $H19^{\Delta 3mat/+}$ male and female obtained were plotted on the figure as an indication of the $H19^{\Delta 3mat/+}$ overgrowth phenotype. $H19^{\Delta 3mat/+;YAC}$ mice were not different from wild-type littermates at birth. The ratio of the weight

of $H19^{\Delta 3mat/+;YAC}$ versus wild-type mice clearly showed that there was no weight difference between these animals (Fig. 2B). As $H19^{\Delta 3mat/+}$ mice are bigger than wild type and as there was no weight difference between $H19^{\Delta 3mat/+;YAC}$ and wild type, we can conclude that the YAC transgene expression on a $H19^{\Delta 3mat/+}$ background rescues the knock-out overgrowth phenotype.

Taken together, these growth curve analyses from two independent lines show for the first time that transgenic *H19* expression leads to the recovery of normal growth on a $H19^{\Delta 3mat/+}$ background. This suggests a role for the *H19* RNA itself in the control of the growth process.

As transgenic mice were smaller at birth, we also checked embryonic growth from E12.5 to E18.5 (see Fig. S1C in the supplementary material). A growth reduction trend between transgenic and control embryos was seen starting at E16.5. We therefore chose to base our expression study at the earlier E14.5 stage, in order to investigate whether a misregulation of growth controlling genes was the cause of this trend.

Control of *H19* expression in transgenic animals

Our aim was to identify targets of the *H19* RNA. Mice were mated to obtain the different genotypes of interest in the same litters, thereby reducing effects due to genetic background heterogeneity. $H19^{\Delta 3/+}$ females were mated with Tg24 males and $H19^{\Delta 3/+};YAC$ females were mated with wild-type males. Wild-type, $H19^{+/+;Tg24}$, $H19^{\Delta 3mat/+}$ and $H19^{\Delta 3mat/+;Tg24}$ littermates, and wild-type, $H19^{+/+;YAC}$, $H19^{\Delta 3mat/+}$ and $H19^{\Delta 3mat/+;YAC}$ littermates, respectively, were obtained (Fig. 3A). All transgenic mice carry a hemizygous allele of the Tg24 or YAC transgene.

In our experiments, we observed a bias in transgene transmission (Fig. 3B). In the Tg24 mating, we obtained only four $H19^{+/+;Tg24}$ mice out of 31 animals from three litters, which corresponds to 13% instead of the expected 25%. For the YAC line, we obtained only one $H19^{+/+;YAC}$ mouse out of 47 animals from four litters, which corresponds to 2% instead of the expected 25%.

H19 expression was then checked by RT-qPCR in the four genotypes. Expression of the transgene was 79% for Tg24 and 88% for YAC on the $H19^{\Delta 3mat/+}$ background (Fig. 3B). Therefore the few transgenic animals obtained on the wild-type background (Tg24 or YAC) would be expected to express *H19* at 179% and 188%, respectively. Interestingly, expression reached only 131% for $H19^{+/+;Tg24}$ and 115% for $H19^{+/+;YAC}$ animals (Fig. 3B), suggesting a bias not only in transgene transmission but also in total *H19* expression. These results are in favour of an as yet unexplained control of the *H19* RNA expression level during embryogenesis.

Igf2 expression analysis

The overgrowth phenotype of $H19^{\Delta 3}$ mice was originally attributed to an overexpression of *Igf2* in mesoderm-derived tissues (Ripoche et al., 1997; Yoshimizu et al., 2008). To investigate whether *Igf2* expression could be directly affected by *H19*, we analyzed *Igf2* expression in E14.5 embryonic muscle tissue (n=4 for each genotype) from the wild-type, $H19^{\Delta 3mat/+}$ and $H19^{\Delta 3mat/+;Tg24}$ littermates and wild-type, $H19^{\Delta 3mat/+}$ and $H19^{\Delta 3mat/+;YAC}$ littermates described in Fig. 3A. RNA was prepared from two embryos per genotype from two different litters (indicated by an asterisk in Fig. 3B). RT-qPCR experiments (Fig. 4) revealed the expected increase in *Igf2* mRNA levels in the $H19^{\Delta 3mat/+}$ samples. Most interestingly, a significantly reduced expression of *Igf2* was detected in both the Tg24 and YAC transgenic samples, with expression being restored to the wild-type level. This suggests that the *H19* RNA itself is involved in the downregulation of *Igf2* mRNA expression by a trans-acting process.

Imprinted gene network (IGN) analysis

In order to investigate whether *Igf2* was the only target of *H19* or if other genes were also affected, hemizygous Tg24 females were mated with $Igf2^{-/-}$ males. We compared the weight of transgenic and non-transgenic littermates and observed that the reduction in weight

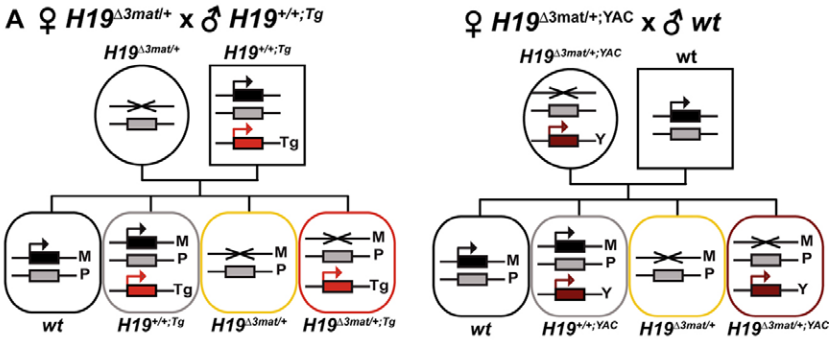

B

$H19^{\Delta 3mat/+}$ females x $H19^{+/+;Tg}$ males

	Litter 1*	Litter 2*	Litter 3		total	%	*H19* expression
wt	3	4	1		8	26%	1.06 ± 0.14 (100%)
$H19^{+/+;Tg}$	**1**	**2**	**1**		**4**	**13%**	**1.39 ± 0.41 (131%)**
$H19^{\Delta 3mat/+}$	5	4	1		10	32%	0.01 ± 0.00 (0%)
$H19^{\Delta 3mat/+;Tg}$	2	2	5		9	29%	0.83 ± 0.11 (79%)
TOTAL	11	12	8		31		

$H19^{\Delta 3mat/+;YAC}$ females x *wt* males

	Litter 1*	Litter 2	Litter 3	Litter 4*	total	%	*H19* expression
wt	4	3	2	8	17	36%	0.93 ± 0.15 (100%)
$H19^{+/+;YAC}$	**0**	**0**	**0**	**1**	**1**	**2%**	**1.07 (115%)**
$H19^{\Delta 3mat/+}$	5	2	2	2	11	24%	0.00 ± 0.00 (0%)
$H19^{\Delta 3mat/+;YAC}$	4	2	6	5	18	38%	0.82 ± 0.29 (88%)
TOTAL	13	8	9	16	47		

Fig. 3. Transgenic matings and transmission. (**A**) Diagram of the two transgenic matings. $H19^{\Delta 3/+}$ females were mated with $H19^{+/+;Tg24+/-}$ males. Because the YAC transgene is imprinted, it had to be transmitted through the female and $H19^{\Delta 3/+;YAC+/-}$ females were mated with wild-type males. Four genotypes are obtained in the same litter: wild type, $H19^{+/+;Tg24}$, $H19^{\Delta 3mat/+}$ and $H19^{\Delta 3mat/+;Tg24}$ for the Tg24 line, and wild type, $H19^{+/+;YAC}$, $H19^{\Delta 3mat/+}$ and $H19^{\Delta 3mat/+;YAC}$ for the YAC line. *H19* gene deletion is represented with a cross and expression with an arrow. M indicates maternal allele, P indicates paternal allele, and Tg and Y indicate Tg24 and YAC transgenes, respectively. (**B**) Distribution of the four genotypes obtained in each mating and associated *H19* RNA levels. A bias in the transmission of the $H19^{+/+;Tg24}$ and $H19^{+/+;YAC}$ was observed, as it is expected to be 25%. The average *H19* expression in E14.5 limb muscle is given for each genotype. Asterisks indicate the litter from which the animals used for the expression analysis originate.

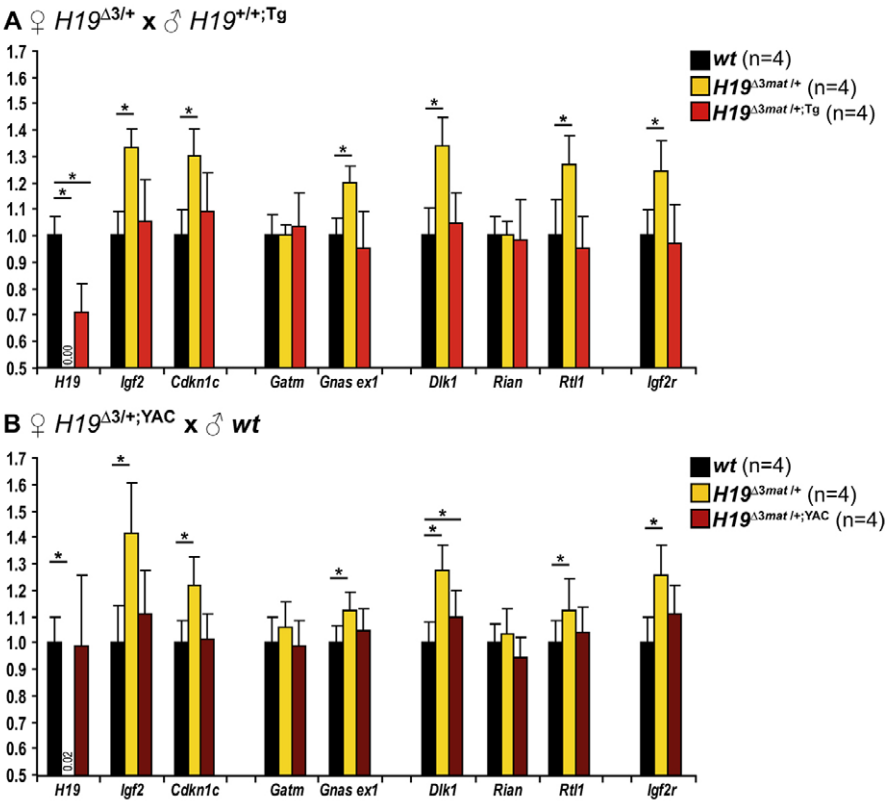

Fig. 4. Imprinted gene network analysis. Expression levels in E14.5 muscle samples were determined by RT-qPCR. The nine genes with significantly similar results between the two transgenic lines are represented. The expression level of wild-type mice was set at 1 and histograms show modifications relative to this level. (**A**) Results obtained with a $H19^{\Delta 3/+} \times H19^{+/+;Tg24+/-}$ mating. (**B**) Results obtained with a $H19^{\Delta 3/+;YAC+/-} \times$wild type mating. Error bars indicate s.e.m. Asterisks indicate significant differences versus the wild-type genotype, as indicated by non-parametric Kruskal-Wallis analysis of variance followed by post-hoc paired comparisons.

could still be detected between these two genotypes (Fig. 5). This indicated that *Igf2* was not the only factor affected by the transgenic expression of *H19*.

H19 and *Igf2* have recently been reported to belong to an imprinted gene network (IGN) (Varrault et al., 2006). We decided to study whether a loss of *H19* function could lead to the deregulation of other genes of the IGN and whether *H19* transgenic expression could rescue this deregulation. We focused on embryonic muscle tissue in which the expression of the transgenes is the strongest (Fig. 1C). For both independent transgenic matings (Fig. 3A), data were generated from four E14.5 embryos for each genotype from two different litters. The results of the RT-qPCR experiments were analyzed with a Kruskal-Wallis one-way analysis of variance test with Benjamini-Hochberg correction and histograms are shown in Fig. 4. As the effect observed was independent of the expression level of each gene, we normalized all data to wild-type expression; a complete table is available in the supplementary material (see Table S1).

We were able to show that six out of twenty genes were significantly upregulated in $H19^{\Delta 3mat/+}$ mice and that five were rescued to wild-type levels in both $H19^{\Delta 3mat/+;Tg24}$ (Fig. 4A) and $H19^{\Delta 3mat/+;YAC}$ embryos (Fig. 4B). The other genes affected besides *Igf2* were *Cdkn1c*, which is located with *H19* on the distal part of mouse chromosome 7, *Gnas* (chromosome 2), *Dlk1* and *Rtl1* (chromosome 12), and *Igf2r* (chromosome 17). Interestingly, the expression of two genes was not modified in either transgenic line: *Gatm* and *Rian*. Moreover, three genes were modulated in the YAC line but were not studied in the Tg24 samples: *Dcn*, *Peg3* and *Slc38a4*. Finally, expression of *Zac1*, which was one of the first genes to be associated with the IGN when it was originally described, remained constant. To summarize, we observed an upregulation of expression of six genes in $H19^{\Delta 3mat/+}$ embryonic muscle tissue, and five of these were restored to the wild-type expression level in the embryos of the two *H19* transgenic lines. In parallel, we also analyzed E14.5 placental RNA from the YAC samples (in which transgenic *H19* RNA is expressed at a level similar to the endogenous level) and found that this IGN control was not present in this extra-embryonic tissue (see Table S2 in the supplementary material).

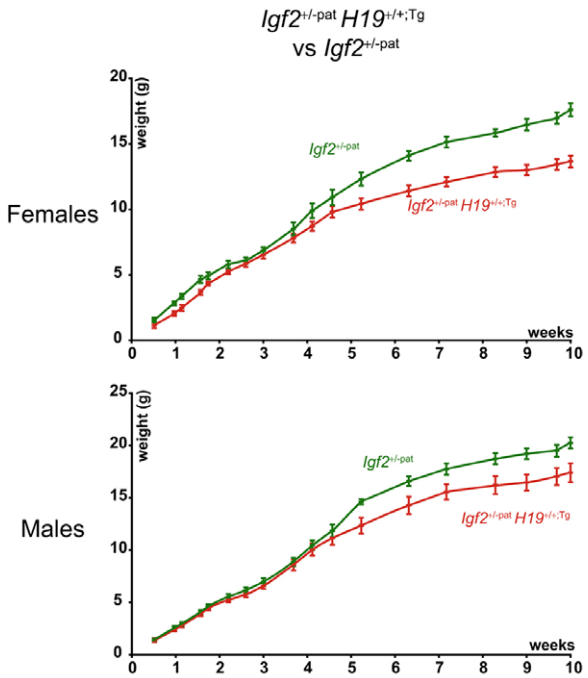

Fig. 5. Growth phenotype of progeny from an $H19^{+/+;Tg24+/-}$ female × an $Igf2^{-/-}$ male. Growth curves for female (top) and male (bottom) littermates correspond to the average of five litters from birth to 10 weeks of age. Error bars indicate s.e.m.

This detailed analysis not only uncovers an effect of the *H19* gene deletion on the expression of several genes, but also demonstrates a trans effect of the *H19* RNA on the mRNA levels of five genes in our two independent transgenic lines. This supports the finding that a functional IGN exists, and suggests that *H19* acts as a regulator of this IGN in the embryo. This is the first in vivo evidence of a functional role for *H19* RNA.

DISCUSSION

Our purpose was to use mouse models to explore in vivo the function of the *H19* non-coding RNA. Targeted deletions of the *H19* gene ($H19^{\Delta 13}$ and $H19^{\Delta 3}$) have lead to overgrowth phenotypes, which can be explained by a cis effect of the *H19* locus on the *Igf2* gene, which becomes biallelically expressed (Leighton et al., 1995; Ripoche et al., 1997). It has, however, been difficult to separate chromatin configuration effects on the locus and a role for the *H19* RNA itself. We therefore decided to produce transgenic animals to express the RNA outside of its own genomic context. We created several transgenic lines expressing the *H19* RNA under the control of the *Ndn* gene promoter. We focused our study on one line, the Tg24 line, as the others showed either low expression of *H19* or mosaicism. We added to our study the previously described YZ8 one-copy YAC transgenic line, with *H19* being expressed under its own promoter (Ainscough et al., 1997). Because these two totally independent lines produced almost identical results, we can exclude any insertional effect due to the transgene. Furthermore, our genetic approach was designed to compare the different genotypes of interest in the same litter, thus limiting the variability of genetic background and maternal effect.

Our first observations lead to the conclusion that, on an $H19^{\Delta 3/\Delta 3}$ background, the *H19* RNA was expressed correctly in both Tg24 and YAC lines, at a level similar to the endogenous level. However, on a wild-type background, overexpression of *H19* only reached 30% at the most, suggesting a control of the total level of expression of *H19*. In addition, a strong bias was found in the transmission of the $H19^{+/+;Tg24}$ and $H19^{+/+;YAC}$ genotypes. Taking these data together with previous observations suggesting a possible deleterious control of the level of transgenic *H19* expression (Ainscough et al., 2000a; Yoo-Warren et al., 1988), we postulate that one of the first targets of *H19* RNA is the *H19* gene itself.

Careful growth curve analysis clearly shows that the *H19* transgenic expression on an $H19^{\Delta 3mat/+}$ background is able, in both transgenic lines, to rescue the $H19^{\Delta 3mat/+}$ overgrowth phenotype, and results in a phenotypical mirror effect between presence and absence of *H19*. Upon close analysis, we observed that *Igf2* expression was reduced in both $H19^{\Delta 3mat/+;Tg24}$ and $H19^{\Delta 3mat/+;YAC}$ embryos compared with $H19^{\Delta 3mat/+}$ embryos. This is the first direct evidence in vivo of an effect of the *H19* RNA on *Igf2* mRNA expression in trans.

Another clue for the implication of *H19* in growth control is that it belongs to the IGN that controls embryonic and postnatal growth (Varrault et al., 2006). This IGN is composed of at least 16 co-expressed imprinted genes, with almost all of these inducing growth phenotypes upon targeted deletion (Fig. 6). A recent study suggests that some of these genes, and among them *H19* and *Igf2*, are important for fetal and early postnatal growth, and that their downregulation contributes to growth deceleration in order to limit body size (Lui et al., 2008). We observed an upregulation of at least six imprinted genes in $H19^{\Delta 3mat/+}$ animals and a recovery of normal expression, comparable to that of wild type, for five of these genes in transgenic *H19*-expressing animals on a $H19^{\Delta 3mat/+}$ background. Interestingly, among the regulated genes, some are maternally expressed (*Cdkn1c*, *Igf2r* and *Dcn*) and others are paternally expressed (*Igf2*, *Dlk1*, *Rtl1*, *Gnas*, *Peg3* and *Slc38a4*; see Fig. 6A).

A

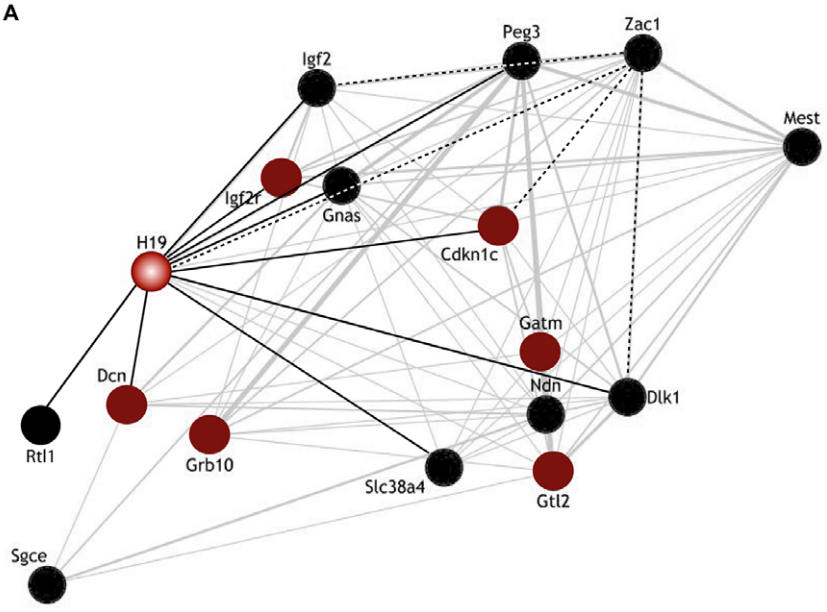

B

	Exp	KO : growth phenotype	Function	Reference
Dlk1	Pat	$+/\Delta pat$: Growth restriction	Delta-like transmembrane and secreted protein, EGF-like family	(Moon *et al.*, 2002)
Gnas	Pat	$+/\Delta pat$: Growth restriction	Gα subunit of G-protein	(Yu *et al.*, 1998)
Igf2	Pat	$+/\Delta pat$: Growth restriction (60% wt)	Embryonic growth factor	(DeChiara *et al.*, 1990)
Peg3	Pat	$+/\Delta pat$: Growth restriction	ZnF protein	(Li *et al.*, 1999)
Rtl1	Pat	Placental defect	Retrotransposon-like protein	(Sekita *et al.*, 2008)
Slc38a4	Pat		Amino acid transporter	
Cdkn1c	Mat	No growth phenotype	Inhibition of cell cycle	(Zhang *et al.*, 1997)
Dcn	Mat	No growth phenotype	Proteoglycan	(Danielson *et al.*, 1997)
Igf2R	Mat	$\Delta mat/+$: overgrowth (140% wt)	*Igf2* clearance	(Wang *et al.*, 1994)

Fig. 6. The imprinted gene network. (**A**) Maternally expressed genes are shown in red and paternally expressed genes in black. Grey lines represent connections between genes as predicted by the original meta-analysis and dotted black lines represent the link between genes found in the *Zac1* study (Varrault et al., 2006). Black lines represent links between *H19* and genes from the present study. (**B**) *H19* regulated genes from the IGN and their effect on growth according to targeted deletion experiments. Six of the regulated genes are paternally expressed and four of them have a positive growth effect. Three are maternally expressed and one has a negative effect on growth.

In agreement with the parental conflict theory (Moore and Haig, 1991), most of the paternally expressed genes have a growth-promoting effect, whereas most of the maternally expressed genes inhibit growth, as shown by their targeted deletion phenotype (Fig. 6B). Our mouse models support the functional existence of the IGN and are in favour of a role for *H19* in its fine-tuned regulation. We hypothesize that by affecting one of the genes of the network, a fully coordinated up or downregulation of oppositely imprinted genes is triggered. This would produce a fine-tuned equilibrium between the interconnected genes of the network, resulting in a compensated growth control and harmonious embryonic development. In fact, our data show that the deregulation of the genes is modest in magnitude, with a maximum significant increase of ~35% for *Igf2* and ~15% for *Gnas*, for example. This hypothesis could also explain the relatively mild phenotype of the $H19^{\Delta 3}$ mice: although *H19* is highly expressed during embryogenesis, targeted deletion of the gene does not result in lethality. This could be due to the triggering of a balance between growth-activating and growth-repressing genes belonging to the IGN.

Interestingly, we did not detect this regulation of the IGN in the placenta of the corresponding embryos, which suggests that regulatory mechanisms differ between extra-embryonic and embryonic tissues, as has been previously shown for X-inactivation or for the *Cdkn1c* locus (Wagschal and Feil, 2006). Further studies of the IGN in the placenta at different times in development might highlight other regulatory aspects of imprinting.

The functional evidence of this IGN raises the question of the mechanism of regulation between these genes. The transcription factor Zac1 is able to bind common enhancers of the *H19* and *Igf2* genes to promote their expression (Varrault et al., 2006). Because *Zac1* is not affected in samples from our study, we can assume it acts upstream from *H19*. Whether several genes of the IGN are direct downstream targets for *H19*, or whether *H19* acts on one gene of the network which then triggers a cascade of events that act on other targets remains to be elucidated. Interactions between imprinted genes have been previously reported, although mechanisms are unclear. A link between *Igf2* and *Cdkn1c* has been described, because an increased circulating Igf2 peptide level in $Igf2r^{-/+}$ animals leads to a decrease of *Cdkn1c* gene expression (Grandjean et al., 2000). In addition, *Igf2r* is a negative regulator of the insulin and IGF signalling pathway (Smith et al., 2006; Wang et al., 1994). We could therefore propose that, in $H19^{\Delta 3mat/+}$ mice, the increased *Igf2* expression might be compensated by *Igf2r* overexpression as a response to maintain overall homeostasis.

Whether a similar IGN exists in human might be of interest to understand some imprinting pathologies. The *H19*/*IGF2* locus is implicated in both Beckwith-Wiedemann syndrome and Silver-Russell syndrome (SRS) (Gicquel et al., 2005). In 60% of SRS patients, hypomethylation of the ICR is observed (Netchine et al., 2007) and could lead to a loss of imprinting of the locus, with loss of *IGF2* expression and *H19* overexpression. However circulating IGF2 peptide levels are found within normal values. Therefore, *H19* overexpression itself could be involved in this syndrome. Other SRS (10%) patients show maternal disomy of chromosome 7, which carries two imprinted loci with *Grb10* and *Sgce*, and *Peg10*, *Mest* and *Copγ2* genes, respectively (Eggermann et al., 1997; Preece et al., 1997). Although our study did not show a significant modulation of *Grb10* or *Mest* mRNA levels, exploring *H19* RNA and IGN expression in SRS patients might help to gain an understanding of how these three loci, which contain functionally different genes, can be linked to the same SRS syndrome.

In our models, we show that *H19* can act in trans to regulate genes of the IGN, which suggests an effect of the RNA itself. This regulation could occur at either the transcriptional or the post-transcriptional level. Two major features arise from an evolutionary conservation study of the *H19* gene: the exon-intron structure of the gene and the precursor of the microRNA miR-675 are conserved, suggesting a role for both the full-length spliced transcript and for the processed miRNA (Smits et al., 2008). The full-length RNA could possibly induce a transcriptional or post-transcriptional control of IGN genes through interactions with chromatin-modifying proteins or with as yet unknown RNA-binding proteins. The post-transcriptional control could also be mediated by miR-675. By binding their mRNA targets in an miRISC complex with an imperfect match, microRNAs are known as translational repressors but they can also lead to mRNA degradation or sequestration in P-bodies (Chu and Rana, 2007). MiR-675 could therefore act directly on the mRNA levels found to be regulated in our mouse models or could indirectly control mRNA stability or the translation of a common regulator. Further experiments will be required to distinguish between the effects of the full-length *H19* RNA and miR-675.

In summary, we have shown with two independent transgenic lines that the *H19* non-coding RNA can act as a trans regulator not only on *Igf2*, but also on several other imprinted genes belonging to an interconnected network involved in the control of growth and survival of mouse embryos. Although the direct or indirect mechanisms involved in this regulation are not yet understood, this opens up new perspectives on the regulatory aspects of genomic imprinting and its function in development and in human pathologies.

Acknowledgements

This paper is dedicated to the memory of Charles Babinet, who was a pioneer in mouse genetics and transgenesis. We are grateful to Arg Efstratiadis for the $Igf2^{-/-}$ mice. We thank Xavier Montagutelli for constant advice on statistical analyses. This work was supported by funding from the Ministère de la Recherche (ACI), Ligue contre le Cancer and the Association Française contre les Myopathies (AFM) to L.D., the Association de la Recherche contre le Cancer (ARC) to both L.D. and T.F., and the ANR Epinet Project to L.J., T.F. and L.D., and by fellowships from the MRT and the ARC to A.G.

Supplementary material

Supplementary material for this article is available at
http://dev.biologists.org/cgi/content/full/136/20/3413/DC1

References

Ainscough, J. F., Koide, T., Tada, M., Barton, S. and Surani, M. A. (1997). Imprinting of *Igf2* and *H19* from a 130 kb YAC transgene. *Development* **124**, 3621-3632.

Ainscough, J. F., Dandolo, L. and Surani, M. A. (2000a). Appropriate expression of the mouse *H19* gene utilises three or more distinct enhancer regions spread over more than 130 kb. *Mech. Dev.* **91**, 365-368.

Ainscough, J. F., John, R. M., Barton, S. C. and Surani, M. A. (2000b). A skeletal muscle-specific mouse *Igf2* repressor lies 40 kb downstream of the gene. *Development* **127**, 3923-3930.

Andrieu, D., Watrin, F., Niinobe, M., Yoshikawa, K., Muscatelli, F. and Fernandez, P. A. (2003). Expression of the Prader-Willi gene Necdin during mouse nervous system development correlates with neuronal differentiation and p75NTR expression. *Gene Expr. Patterns* **3**, 761-765.

Barsyte-Lovejoy, D., Lau, S. K., Boutros, P. C., Khosravi, F., Jurisica, I., Andrulis, I. L., Tsao, M. S. and Penn, L. Z. (2006). The c-Myc oncogene directly induces the *H19* noncoding RNA by allele-specific binding to potentiate tumorigenesis. *Cancer Res.* **66**, 5330-5337.

Bartolomei, M. S., Zemel, S. and Tilghman, S. M. (1991). Parental imprinting of the mouse *H19* gene. *Nature* **351**, 153-155.

Brannan, C. I., Dees, E. C., Ingram, R. S. and Tilghman, S. M. (1990). The product of the *H19* gene may function as an RNA. *Mol. Cell. Biol.* **10**, 28-36.

Cai, X. and Cullen, B. R. (2007). The imprinted *H19* noncoding RNA is a primary microRNA precursor. *RNA* **13**, 313-316.

Chu, C. Y. and Rana, T. M. (2007). Small RNAs: regulators and guardians of the genome. *J. Cell Physiol.* **213**, 412-419.

Danielson, K. G., Baribault, H., Holmes, D. F., Graham, H., Kadler, K. E. and Iozzo, R. V. (1997). Targeted disruption of decorin leads to abnormal collagen fibril morphology and skin fragility. *J. Cell Biol.* **136**, 729-743.
Dao, D., Walsh, C. P., Yuan, L., Gorelov, D., Feng, L., Hensle, T., Nisen, P., Yamashiro, D. J., Bestor, T. H. and Tycko, B. (1999). Multipoint analysis of human chromosome 11p15/mouse distal chromosome **7**, inclusion of *H19/IGF2* in the minimal WT2 region, gene specificity of *H19* silencing in Wilms' tumorigenesis and methylation hyper-dependence of *H19* imprinting. *Hum. Mol. Genet.* **8**, 1337-1352.
DeChiara, T. M., Efstratiadis, A. and Robertson, E. J. (1990). A growth-deficiency phenotype in heterozygous mice carrying an *insulin-like growth factor II* gene disrupted by targeting. *Nature* **345**, 78-80.
DeChiara, T. M., Robertson, E. J. and Efstratiadis, A. (1991). Parental imprinting of the mouse *insulin-like growth factor II* gene. *Cell* **64**, 849-859.
Eggermann, T., Wollmann, H. A., Kuner, R., Eggermann, K., Enders, H., Kaiser, P. and Ranke, M. B. (1997). Molecular studies in 37 Silver-Russell syndrome patients: frequency and etiology of uniparental disomy. *Hum. Genet.* **100**, 415-419.
Forne, T., Oswald, J., Dean, W., Saam, J. R., Bailleul, B., Dandolo, L., Tilghman, S. M., Walter, J. and Reik, W. (1997). Loss of the maternal *H19* gene induces changes in *Igf2* methylation in both *cis* and *trans*. *Proc. Natl. Acad. Sci. USA* **94**, 10243-10248.
Frevel, M. A., Sowerby, S. J., Petersen, G. B. and Reeve, A. E. (1999). Methylation sequencing analysis refines the region of *H19* epimutation in Wilms tumor. *J. Biol. Chem.* **274**, 29331-29340.
Gabory, A., Ripoche, M. A., Yoshimizu, T. and Dandolo, L. (2006). The *H19* gene: regulation and function of a non-coding RNA. *Cytogenet. Genome Res.* **113**, 188-193.
Gicquel, C., Rossignol, S., Cabrol, S., Houang, M., Steunou, V., Barbu, V., Danton, F., Thibaud, N., Le Merrer, M., Burglen, L. et al. (2005). Epimutation of the telomeric imprinting center region on chromosome 11p15 in Silver-Russell syndrome. *Nat. Genet.* **37**, 1003-1007.
Grandjean, V., Smith, J., Schofield, P. N. and Ferguson-Smith, A. C. (2000). Increased IGF-II protein affects p57kip2 expression in vivo and in vitro: implications for Beckwith-Wiedemann syndrome. *Proc. Natl. Acad. Sci. USA* **97**, 5279-5284.
Hao, Y., Crenshaw, T., Moulton, T., Newcomb, E. and Tycko, B. (1993). Tumour-suppressor activity of *H19* RNA. *Nature* **365**, 764-767.
Hark, A. T., Schoenherr, C. J., Katz, D. J., Ingram, R. S., Levorse, J. M. and Tilghman, S. M. (2000). CTCF mediates methylation-sensitive enhancer-blocking activity at the *H19/Igf2* locus. *Nature* **405**, 486-489.
Juan, V., Crain, C. and Wilson, C. (2000). Evidence for evolutionarily conserved secondary structure in the *H19* tumor suppressor RNA. *Nucleic Acids Res.* **28**, 1221-1227.
Kuo, C. H., Uetsuki, T., Kim, C. H., Tanaka, H., Li, B. S., Taira, E., Higuchi, H., Okamoto, H., Yoshikawa, K. and Miki, N. (1995). Determination of a necdin cis-acting element required for neuron specific expression by using zebra fish. *Biochem. Biophys. Res. Commun.* **211**, 438-446.
Leighton, P. A., Ingram, R. S., Eggenschwiler, J., Efstratiadis, A. and Tilghman, S. M. (1995). Disruption of imprinting caused by deletion of the *H19* gene region in mice. *Nature* **375**, 34-39.
Li, L., Keverne, E. B., Aparicio, S. A., Ishino, F., Barton, S. C. and Surani, M. A. (1999). Regulation of maternal behavior and offspring growth by paternally expressed Peg3. *Science* **284**, 330-333.
Li, Y. M., Franklin, G., Cui, H. M., Svensson, K., He, X. B., Adam, G., Ohlsson, R. and Pfeifer, S. (1998). The *H19* transcript is associated with polysomes and may regulate *IGF2* expression in trans. *J. Biol. Chem.* **273**, 28247-28252.
Lui, J. C., Finkielstain, G. P., Barnes, K. M. and Baron, J. (2008). An imprinted gene network that controls mammalian somatic growth is down-regulated during postnatal growth deceleration in multiple organs. *Am. J. Physiol. Regul. Integr. Comp. Physiol.* **295**, R189-R196.
Matouk, I. J., DeGroot, N., Mezan, S., Ayesh, S., Abu-lail, R., Hochberg, A. and Galun, E. (2007). The *H19* non-coding RNA is essential for human tumor growth. *PLoS ONE* **2**, e845.
Milligan, L., Antoine, E., Bisbal, C., Weber, M., Brunel, C., Forne, T. and Cathala, G. (2000). H19 gene expression is up-regulated exclusively by stabilization of the RNA during muscle cell differentiation. *Oncogene* **19**, 5810-5816.
Mineno, J., Okamoto, S., Ando, T., Sato, M., Chono, H., Izu, H., Takayama, M., Asada, K., Mirochnitchenko, O., Inouye, M. et al. (2006). The expression profile of microRNAs in mouse embryos. *Nucleic Acids Res.* **34**, 1765-1771.
Moon, Y. S., Smas, C. M., Lee, K., Villena, J. A., Kim, K. H., Yun, E. J. and Sul, H. S. (2002). Mice lacking paternally expressed *Pref-1/Dlk1* display growth retardation and accelerated adiposity. *Mol. Cell. Biol.* **22**, 5585-5592.
Moore, T. and Haig, D. (1991). Genomic imprinting in mammalian development: a parental tug-of-war. *Trends Genet.* **7**, 45-49.
Netchine, I., Rossignol, S., Dufourg, M. N., Azzi, S., Rousseau, A., Perin, L., Houang, M., Steunou, V., Esteva, B., Thibaud, N. et al. (2007). 11p15 imprinting center region 1 loss of methylation is a common and specific cause of typical Russell-Silver syndrome: clinical scoring system and epigenetic-phenotypic correlations. *J. Clin. Endocrinol. Metab.* **92**, 3148-3154.
Pachnis, V., Brannan, C. I. and Tilghman, S. M. (1988). The structure and expression of a novel gene activated in early mouse embryogenesis. *EMBO J.* **7**, 673-681.
Poirier, F., Chan, C. T., Timmons, P. M., Robertson, E. J., Evans, M. J. and Rigby, P. W. (1991). The murine *H19* gene is activated during embryonic stem cell differentiation in vitro and at the time of implantation in the developing embryo. *Development* **113**, 1105-1114.
Preece, M. A., Price, S. M., Davies, V., Clough, L., Stanier, P., Trembath, R. C. and Moore, G. E. (1997). Maternal uniparental disomy 7 in Silver-Russell syndrome. *J. Med. Genet.* **34**, 6-9.
Ripoche, M. A., Kress, C., Poirier, F. and Dandolo, L. (1997). Deletion of the *H19* transcription unit reveals the existence of a putative imprinting control element. *Genes Dev.* **11**, 1596-1604.
Sekita, Y., Wagatsuma, H., Nakamura, K., Ono, R., Kagami, M., Wakisaka, N., Hino, T., Suzuki-Migishima, R., Kohda, T., Ogura, A. et al. (2008). Role of retrotransposon-derived imprinted gene, Rtl1, in the feto-maternal interface of mouse placenta. *Nat. Genet.* **40**, 243-248.
Smith, F. M., Garfield, A. S. and Ward, A. (2006). Regulation of growth and metabolism by imprinted genes. *Cytogenet. Genome Res.* **113**, 279-291.
Smits, G., Mungall, A. J., Griffiths-Jones, S., Smith, P., Beury, D., Matthews, L., Rogers, J., Pask, A. J., Shaw, G., VandeBerg, J. L. et al. (2008). Conservation of the *H19* non-coding RNA and *H19-Igf2* imprinting mechanism in therians. *Nat. Genet.* **40**, 971-976.
Thorvaldsen, J. L., Duran, K. L. and Bartolomei, M. S. (1998). Deletion of the *H19* differentially methylated domain results in loss of imprinted expression of *H19* and *Igf2*. *Genes Dev.* **12**, 3693-3702.
Vandesompele, J., De Preter, K., Pattyn, F., Poppe, B., Van Roy, N., De Paepe, A. and Speleman, F. (2002). Accurate normalization of real-time quantitative RT-PCR data by geometric averaging of multiple internal control genes. *Genome Biol.* **3**, RESEARCH0034.
Varrault, A., Gueydan, C., Delalbre, A., Bellmann, A., Houssami, S., Aknin, C., Severac, D., Chotard, L., Kahli, M., Le Digarcher, A. et al. (2006). Zac1 regulates an imprinted gene network critically involved in the control of embryonic growth. *Dev. Cell* **11**, 711-722.
Wagschal, A. and Feil, R. (2006). Genomic imprinting in the placenta. *Cytogenet. Genome Res.* **113**, 90-98.
Wang, Z. Q., Fung, M. R., Barlow, D. P. and Wagner, E. F. (1994). Regulation of embryonic growth and lysosomal targeting by the imprinted *Igf2/Mpr* gene. *Nature* **372**, 464-467.
Wilkin, F., Paquette, J., Ledru, E., Hamelin, C., Pollak, M. and Deal, C. L. (2000). *H19* sense and antisense transgenes modify *insulin-like growth factor-II* mRNA levels. *Eur. J. Biochem.* **267**, 4020-4027.
Yoo-Warren, H., Pachnis, V., Ingram, R. S. and Tilghman, S. M. (1988). Two regulatory domains flank the mouse *H19* gene. *Mol. Cell. Biol.* **8**, 4707-4715.
Yoshimizu, T., Miroglio, A., Ripoche, M. A., Gabory, A., Vernucci, M., Riccio, A., Colnot, S., Godard, C., Terris, B., Jammes, H. et al. (2008). The *H19* locus acts *in vivo* as a tumour suppressor. *Proc. Natl. Acad. Sci. USA* **105**, 12417-12422.
Yu, S., Yu, D., Lee, E., Eckhaus, M., Lee, R., Corria, Z., Accili, D., Westphal, H. and Weinstein, L. S. (1998). Variable and tissue-specific hormone resistance in heterotrimeric Gs protein alpha-subunit (Gsalpha) knockout mice is due to tissue-specific imprinting of the gsalpha gene. *Proc. Natl. Acad. Sci. USA* **95**, 8715-8720.
Zemel, S., Bartolomei, M. S. and Tilghman, S. M. (1992). Physical linkage of two mammalian imprinted genes, *H19* and *insulin-like growth factor 2*. *Nat. Genet.* **2**, 61-65.
Zhang, P., Liegeois, N. J., Wong, C., Finegold, M., Hou, H., Thompson, J. C., Silverman, A., Harper, J. W., DePinho, R. A. and Elledge, S. J. (1997). Altered cell differentiation and proliferation in mice lacking p57KIP2 indicates a role in Beckwith-Wiedemann syndrome. *Nature* **387**, 151-158.
Zhang, Y. and Tycko, B. (1992). Monoallelic expression of the human *H19* gene. *Nat. Genet.* **1**, 40-44.

Table S1. Complete results of the IGN network analysis from E14.5 limb muscle

Cross	♀ $H19^{\Delta 3mat/+}$ x ♂ $H19^{+/+;Tg}$										♀ $H19^{\Delta 3mat/+;YAC}$ x ♂ *wt*									
Genotype	***WT***		***H19$^{\Delta 3mat/+}$***				***H19$^{\Delta 3mat/+;Tg}$***				***WT***		***H19$^{\Delta 3mat/+}$***				***H19$^{\Delta 3mat/+;YAC}$***			
Gene name	**Average**	**sd**	**Average**	**sd**	**KO/WT**	**Signif.**	**Average**	**sd**	**KOTg/ WT**	**Signif.**	**Average**	**sd**	**Average**	**sd**	**KO/WT**	**Signif.**	**Average**	**sd**	**KOYac/ WT**	**Signif.**
Cdkn1c	**29.33**	**5.55**	**38.14**	**5.80**	**1.30**	**+**	**31.97**	**8.75**	**1.09**	**-**	**57.52**	**10.01**	**70.09**	**12.15**	**1.22**	**+**	**58.35**	**10.69**	**1.01**	**-**
Dcn	/	/	/	/			/	/			**6.62**	**1.07**	**7.38**	**1.19**	**1.11**	**+**	**6.64**	**1.25**	**1.00**	**-**
Dlk1	**22.94**	**4.85**	**30.73**	**4.87**	**1.34**	**+**	**23.95**	**5.37**	**1.04**	**-**	**26.41**	**4.21**	**33.60**	**5.06**	**1.27**	**+**	**28.96**	**5.31**	**1.10**	**+**
Gatm	0.42	0.06	0.42	0.03	1.00	-	0.43	0.11	1.03	-	0.50	0.09	0.53	0.09	1.06	-	0.50	0.09	0.99	-
Gnas ex1	**16.02**	**2.15**	**19.25**	**1.97**	**1.20**	**+**	**15.23**	**4.49**	**0.95**	**-**	**26.03**	**3.34**	**29.26**	**3.44**	**1.12**	**+**	**27.27**	**4.35**	**1.05**	**-**
Gnas XL	2.36	0.31	3.21	0.52	1.36	+	2.32	0.64	0.98	-	2.30	0.39	2.69	0.37	1.17	-	2.43	0.66	1.06	-
Gtl2	20.11	3.16	24.77	4.35	1.23	+	18.53	6.26	0.92	-	11.37	1.77	11.20	2.13	0.98	-	12.07	3.27	1.06	-
Grb10	6.19	0.88	7.49	1.01	1.21	+	5.98	2.18	0.97	-	8.13	1.23	8.89	1.65	1.09	-	8.44	1.46	1.04	-
H19	265.37	37.71	0.27	0.13	0.00	+	188.47	56.14	0.71	+	215.43	42.50	4.75	11.24	0.02	+	213.35	113.45	0.99	+
Igf2	**102.29**	**17.93**	**135.93**	**14.81**	**1.33**	**+**	**107.93**	**32.07**	**1.06**	**-**	**64.49**	**17.86**	**91.28**	**24.00**	**1.42**	**+**	**71.38**	**21.93**	**1.11**	**-**
Igf2r	**1.72**	**0.34**	**2.13**	**0.40**	**1.24**	**+**	**1.67**	**0.49**	**0.97**	**-**	**0.66**	**0.13**	**0.84**	**0.15**	**1.26**	**+**	**0.73**	**0.14**	**1.11**	**-**
Mest	10.37	1.91	13.26	1.73	1.28	+	9.90	3.43	0.95	-	7.29	2.19	8.28	2.70	1.14	-	7.48	2.62	1.03	-
Ndn	/	/	/	/			/	/			1.58	0.39	1.56	0.40	0.99	-	1.53	0.46	0.97	-
Peg3	/	/	/	/			/	/			**17.93**	**2.33**	**19.84**	**2.88**	**1.11**	**+**	**18.47**	**2.89**	**1.03**	**-**
Rian	16.03	2.26	16.02	1.59	1.00	-	15.79	4.85	0.99	-	9.96	1.43	10.27	1.93	1.03	-	9.43	1.42	0.95	-
Rtl1	**0.27**	**0.07**	**0.34**	**0.06**	**1.27**	**+**	**0.25**	**0.07**	**0.95**	**-**	**0.41**	**0.07**	**0.47**	**0.10**	**1.13**	**+**	**0.43**	**0.08**	**1.04**	**-**
Slc38a4	/	/	/	/			/	/			**1.52**	**0.32**	**1.81**	**0.52**	**1.19**	**+**	**1.63**	**0.50**	**1.07**	**-**
Zac1	/	/	/	/			/	/			5.80	1.32	6.28	1.84	1.08	-	5.52	1.64	0.95	-

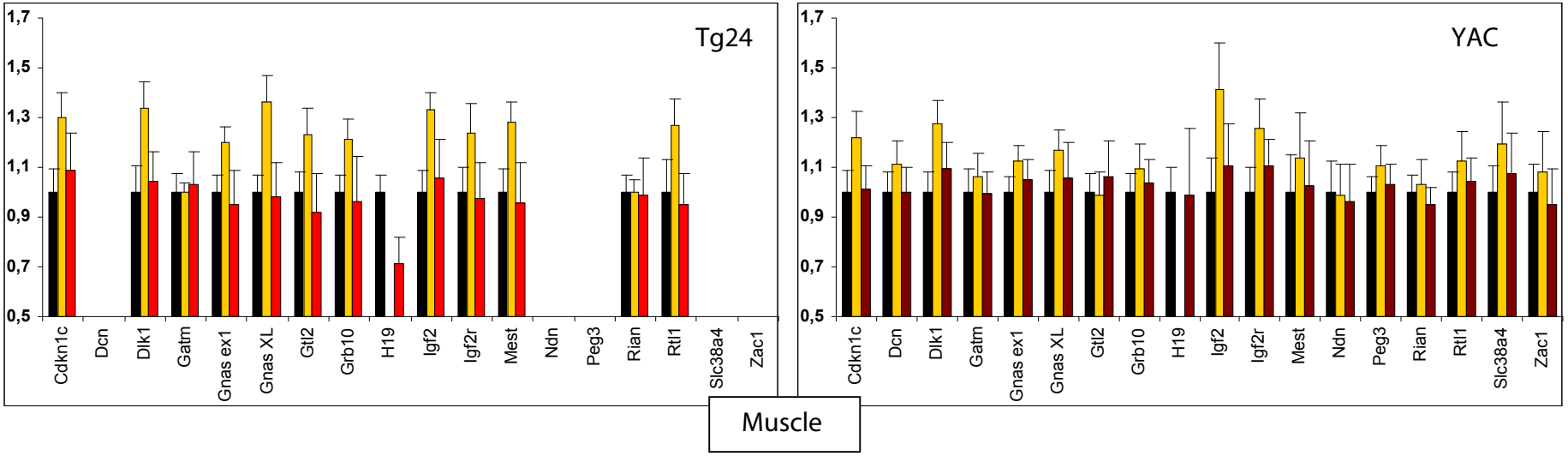

Table S2. Complete results of the IGN network analysis from E14.5 placenta

Cross	♀ $H19^{\Delta 3mat/+}$ x ♂ $H19^{+/+;Tg}$										♀ $H19^{\Delta 3mat/+;YAC}$ x ♂ *wt*									
Genotype	***WT***		***H19$^{\Delta 3mat/+}$***				***H19$^{\Delta 3mat/+;Tg}$***				***WT***		***H19$^{\Delta 3mat/+}$***				***H19$^{\Delta 3mat/+;YAC}$***			
Gene name	**Average**	**sd**	**Average**	**sd**	**KO/WT**	**Signif.**	**Average**	**sd**	**KOTg/ WT**	**Signif.**	**Average**	**sd**	**Average**	**sd**	**KO/WT**	**Signif.**	**Average**	**sd**	**KOYac/ WT**	**Signif.**
Cdkn1c	2.32	0.47	2.46	0.51	1.06		2.58	0.35	1.11		50.79	9.16	54.84	6.06	1.08		51.18	10.84	1.01	
Dcn	/	/	/	/			/	/			18.32	3.45	17.43	4.31	0.95		14.07	2.75	0.77	
Dlk1	0.65	0.07	0.58	0.15	0.89		0.68	0.15	1.03		5.43	2.02	4.65	2.36	0.86		6.41	1.02	1.18	
Gatm	0.48	0.14	0.45	0.13	0.93		0.39	0.07	0.81		6.07	1.28	5.74	1.95	0.95		4.65	1.47	0.77	
Gnas ex1	1.79	0.29	1.76	0.14	0.99		1.72	0.16	0.96		19.74	2.37	16.97	3.60	0.86		22.01	2.31	1.12	
Gnas XL	0.02	0.00	0.02	0.01	1.16		0.02	0.01	1.21		0.11	0.04	0.11	0.04	1.03		0.14	0.03	1.32	
Gtl2	0.51	0.07	0.51	0.20	0.99		0.52	0.16	1.01		2.01	0.66	1.67	0.85	0.83		2.29	0.43	1.14	
Grb10	0.20	0.04	0.19	0.03	0.94		0.23	0.05	1.14		3.00	0.56	2.99	0.54	1.00		2.86	0.61	0.95	
H19	57.85	7.82	0.39	0.15	0.01	+	5.00	0.72	0.09	+	338.25	62.11	3.18	1.66	0.01	+	311.88	75.16	0.92	+
Igf2	10.31	1.35	10.45	1.44	1.01		12.09	1.58	1.17		51.63	12.68	53.29	14.13	1.03		64.20	10.61	1.24	
Igf2r	0.21	0.04	0.20	0.03	0.95		0.22	0.05	1.05		0.42	0.07	0.47	0.08	1.11		0.50	0.08	1.19	
Mest	0.18	0.02	0.18	0.06	0.99		0.21	0.04	1.17		1.83	0.59	1.93	0.59	1.05		1.80	0.42	0.99	
Ndn	/	/	/	/			/	/			0.34	0.08	0.31	0.05	0.91		0.28	0.08	0.82	
Peg3	/	/	/	/			/	/			28.46	3.09	29.98	4.79	1.05		35.23	4.39	1.24	
Rian	0.36	0.06	0.34	0.14	0.96		0.40	0.09	1.10		1.69	0.68	1.65	0.32	0.97		1.49	0.35	0.88	
Rtl1	0.02	0.00	0.02	0.00	0.93		0.02	0.01	1.13		0.41	0.15	0.43	0.14	1.04		0.46	0.09	1.12	
Slc38a4	/	/	/	/			/	/			27.30	3.87	29.23	4.31	1.07		30.88	3.80	1.13	
Zac1	/	/	/	/			/	/			1.95	0.62	1.93	0.58	0.99		2.27	0.53	1.16